This article was downloaded by:
On: *30 January 2011*
Access details: *Access Details: Free Access*
Publisher *Taylor & Francis*
Informa Ltd Registered in England and Wales Registered Number: 1072954 Registered office: Mortimer House, 37-41 Mortimer Street, London W1T 3JH, UK

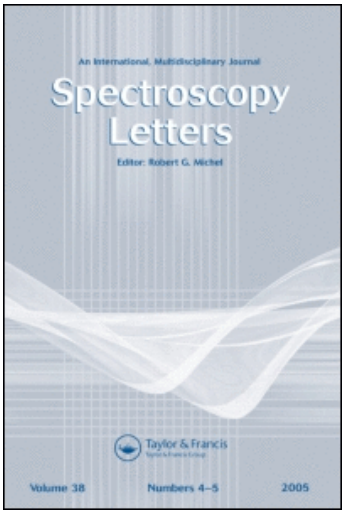

Spectroscopy Letters
Publication details, including instructions for authors and subscription information:
http://www.informaworld.com/smpp/title~content=t713597299

Excitation Mechanisms of Copper Ionic and Atomic Lines Emitted from a Low-Pressure Argon Laser-Induced Plasma

Yohei Ushirozawa[a]; Kazuaki Wagatsuma[a]
[a] Institute for Materials Research, Tohoku University, Sendai, Japan

To cite this Article Ushirozawa, Yohei and Wagatsuma, Kazuaki(2005) 'Excitation Mechanisms of Copper Ionic and Atomic Lines Emitted from a Low-Pressure Argon Laser-Induced Plasma', Spectroscopy Letters, 38: 4, 539 — 555
To link to this Article: DOI: 10.1081/SL-200062947
URL: http://dx.doi.org/10.1081/SL-200062947

PLEASE SCROLL DOWN FOR ARTICLE

Full terms and conditions of use: http://www.informaworld.com/terms-and-conditions-of-access.pdf

This article may be used for research, teaching and private study purposes. Any substantial or systematic reproduction, re-distribution, re-selling, loan or sub-licensing, systematic supply or distribution in any form to anyone is expressly forbidden.

The publisher does not give any warranty express or implied or make any representation that the contents will be complete or accurate or up to date. The accuracy of any instructions, formulae and drug doses should be independently verified with primary sources. The publisher shall not be liable for any loss, actions, claims, proceedings, demand or costs or damages whatsoever or howsoever caused arising directly or indirectly in connection with or arising out of the use of this material.

Spectroscopy Letters, 38: 539–555, 2005
Copyright © Taylor & Francis, Inc.
ISSN 0038-7010 print/1532-2289 online
DOI: 10.1081/SL-200062947

Taylor & Francis
Taylor & Francis Group

Excitation Mechanisms of Copper Ionic and Atomic Lines Emitted from a Low-Pressure Argon Laser-Induced Plasma

Yohei Ushirozawa and Kazuaki Wagatsuma
Institute for Materials Research, Tohoku University, Sendai, Japan

Downloaded At: 03:00 30 January 2011

Abstract: Low-pressure laser-induced plasmas generated with a pulsed Nd: YAG laser have complicated structures both temporally and spatially. The emission characteristics of the plasma are investigated for optimizing the experimental parameters in atomic emission spectrometry. The emission intensities of copper emission lines, measured in a time-resolved as well as a time-integrated mode, are strongly dependent on the kind of copper lines, ionic or atomic line, and the excitation energy. Also, the pressure of argon gas is the most important parameter for determining the behavior of these emission lines, including argon lines. Generally, copper ionic lines are dominantly emitted from the initial breakdown zone, because the copper ions are produced mainly in the hot breakdown zone. However, the Cu II 229.44-nm line is emitted also from the expansion zone of the plasma. It results from an additional excitation process through the charge-transfer collision particularly effective for the corresponding excited level. In this work, the excitation mechanisms for Cu I, Ar I, and Ar II lines are also discussed. The excitations occurring in the laser-induced plasma can be well understood by taking the temporal and spatial variations in their intensities into consideration.

Keywords: Copper emission lines, atomic emission spectroscopy, excitation mechanism, low-pressure laser-induced plasma

INTRODUCTION

Laser-induced plasma spectrometry (LIPS) is a promising technique for direct analysis of various materials because of the rapid response without any sample

Received 2 September 2004, Accepted 3 February 2005
Address correspondence to Kazuaki Wagatsuma, Institute for Materials Research, Tohoku University, Katahira 2-1-1, Sendai 980-8577, Japan. E-mail: wagatuma@imr.tohoku.ac.jp

pre-treatment.[1–10] A Q-switched Nd:YAG laser is irradiated onto the sample surface during a very short period but with a large power density, which produces a pulsed laser-induced plasma (LIP) following the frequency of the laser. Sample atoms are ejected from the surface due to laser ablation and are subsequently ionized and excited in LIP, so that this created plasma has been employed as an excitation source in atomic emission spectrometry.

Plasmas, induced with a Q-switched Nd: YAG laser, have both spatial and temporal characteristics depending on various experimental parameters, such as the kind and the pressure of plasma gas, which is generally referred as an expansion of the plasma plume. The emission zone varies with the progress of the plasma plume, which is strongly dependent on the nature of plasma gas. Further, one has to consider that major processes for the excitations vary also at different portions of the plasma plume. Therefore, in the emission spectrometric application, the optimization for the operating conditions requires different idea of that for inductively coupled radio-frequency plasmas or glow discharge plasmas (GDP). It is known that laser-induced plasmas produced under an evacuated atmosphere have favorable features for emission analysis due to relatively low fluctuation of the emission intensities as well as the high signal-to-background ratio.[11–15]

Downloaded At: 03:00 30 January 2011

The excitation mechanisms of the low-pressure laser-induced plasma (LP-LIP) cannot be fully understood, as the structure of LP-LIP is much complicated both spatially and temporally. Knowledge about the excitations occurring in LP-LIP should be required for optimizing the experimental conditions for the analytical application. Several papers have suggested a possible excitation process caused by a shock wave[12,16] in the front of the plasma plume and a collisional excitation process with metastable species of the plasma gas.[16] Gas species having a long lifetime, such as the metastable atoms and the ground-state ions, may be populated under evacuated conditions in LP-LIP. It is because their de-excitation or recombination occurs less actively under reduced pressures, which is very similar to the environment in a GDP.[17] It is therefore interesting to compare the spectral pattern emitted from LP-LIP with that from GDP. As it has been published in several papers discussing the excitation mechanism in GDP,[18–21] particular ionic lines are excited selectively through (quasi-) resonance charge transfer collisions[22] between a ground-state ion of plasma gas and a ground-state atom of the sample. This reaction can produce a highly populated excited state of the species in the sample, which results in strong emission of particular emission lines resulting from the de-excitation.[23,24]

Our previous paper has reported on a comparison in the spectra of copper both excited from LP-LIP and from GDP when several plasma gases was used.[25,26] It indicated that intense ionic lines of copper observed in GDP were also found in the spectrum from LP-LIP. It implies the similarity in the excitation mechanisms between in LP-LIP and in GDP.[26] In this study, we investigated intensity variations of various copper lines along with the duration time after laser irradiation at different portions of the plasma, in

order to discuss the excitation mechanism in more detail. Their emission intensities are expected to have any different dependence in the progress of the plasma expansion, thus yielding useful information on the excitation mechanisms.

EXPERIMENTAL

A schematic diagram of the apparatus is shown in Fig. 1. A Nd : YAG laser (LOTIS TII LS-2135, Tokyo, Japan) was employed at the wavelength of 532 nm (SHG mode). The laser having the energy of 40 mJ/pulse was irradiated on the sample surface (the spot size of about 0.7 mm in diameter). The pulse duration of about 10 ns and the repetition rate of 10 Hz were employed. A spherical lens with a 200-mm focal length was used to focus the laser pulses onto the target surface. High-purity copper plates (99.999%) were used as sample. The sample plate was polished with waterproof abrasive papers and then fixed at the sample port of the chamber. After the surface was cleaned using the first 100 laser shots, the emission signal was accumulated in the detector during the next 10 shots and recorded in a personal computer.

High-purity argon (99.9995%) was introduced as plasma gas after the evacuation of the chamber below 7 Pa. The pressure was monitored with a Pirani gauge (GP-2, ULVAC Corp., Chigasaki, Japan) and a capacitance manometer (MK 113B-2-P and 127AA-001003, NKS Instruments Inc., Andover, MA, USA) placed between the evacuation port and a rotary vacuum pump (GLD-166, ULVAC Engineering Inc., Chigasaki, Japan). Energy of the pulsed laser was measured using a thermopile absorber head and a laser power/energy monitor (OPHIR JAPAN 3A-P-CAL, NOVA, Tokyo, Japan).

Emission signals, collected directly by an optical fiber, were measured by a spectrograph (Solar TII MS-3504, Tokyo, Japan) equipped with an intensified charge-coupled device detector (ICCD) (Model DH 501, Andor Technology,

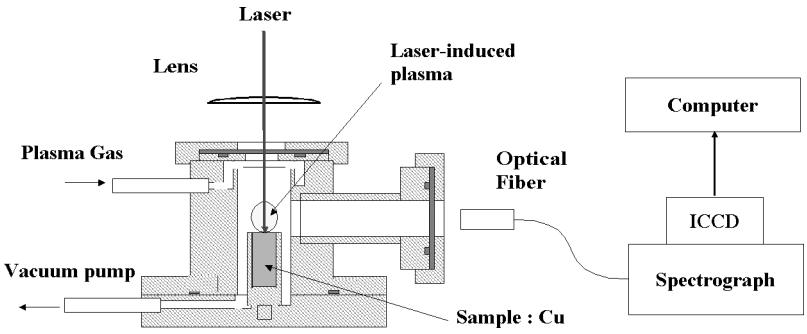

Figure 1. Schematic diagram of the experimental apparatus.

Downloaded At: 03:00 30 January 2011

South Windsor, CT, USA). The spectral resolution was about 0.1 nm when the slit width was set at 30 μm. The optical fiber was placed in front of the observation window of the chamber, so that the observation point was about 5 mm above the sample surface. The distance between the fiber port and the plasma plume was set to be 45 mm. The numerical aperture of the fiber optics was 0.22 and the acceptance angle was about 12.5°. As illustrated in Fig. 2, this arrangement allowed a whole plasma image to be observed over the range of 0–15 mm in height above the sample surface and to have a spatially integrated spectrum. Using this optical alignment, time-integrated spectra were recorded for the period of 0.5 ms (gate width) after an initial delay time of 0.036×10^{-6} s. This initial delay was employed to avoid influence from the laser scattered light and the initial broadband background from the LIP. In this measurement, we employed a cylinder having the height of 5 mm above the sample surface as a blind, as shown in Fig. 2b, in order to eliminate the emission signals originated from the initial breakdown zone. The integrated emission spectra were measured both with and without the blind cylinder. In addition, a series of time-resolved spectra were monitored at the interval

Downloaded At: 03:00 30 January 2011

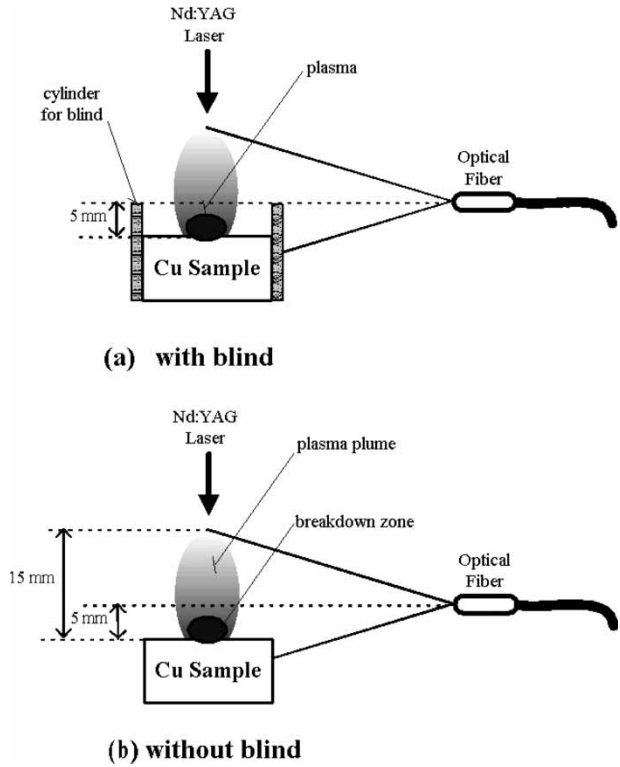

Figure 2. Setup of the measuring system having a cylinder blind.

of 0.24×10^{-6} s (gate width) after any delay time in the range of 0.36×10^{-6} to 5.0×10^{-6} s.

RESULTS AND DISCUSSION

Excitations in LP-LIP

A hot breakdown zone is produced near the sample surface immediately after laser irradiation. Because of direct coupling with the laser having a very high power, the sample materials are ablated and then excited and ionized through various collisions among highly-energetic particles in the breakdown zone. If the sample is pure copper in an argon LP-LIP, the following reactions can be considered:

$$\begin{aligned} \mathrm{Cu} &\rightarrow \mathrm{Cu}^{+} \rightarrow \mathrm{Cu}^{z+} \\ \mathrm{Ar} &\rightarrow \mathrm{Ar}^{+} \rightarrow \mathrm{Ar}^{z+} \end{aligned} \tag{1}$$

Also, various recombination reactions take place simultaneously: for example,

$$\begin{aligned} \mathrm{Ar}^{+} + \mathrm{e}^{-} &\rightarrow \mathrm{Ar}^{*}+)\Delta\mathrm{E} \\ \mathrm{Cu}^{+} + \mathrm{e}^{-} &\rightarrow \mathrm{Cu}^{*}+)\Delta\mathrm{E} \end{aligned} \tag{2}$$

These reactions produce excited species of argon and copper, denoted by Ar^{*} and Cu^{*}, as well as the continuum background over a wide wavelength range. On the other hand, these excited species are also produced through direct collisional excitations: for example,

$$\begin{aligned} \mathrm{Ar} + \mathrm{e}^{-}(\text{ fast}) \text{ or } \mathrm{M}\ (\text{fast}) &\rightarrow \mathrm{Ar}^{*} + \mathrm{e}^{-}(\text{slow}) \text{ or } \mathrm{M}\ (\text{slow}) \\ \mathrm{Cu} + \mathrm{e}^{-}(\text{ fast}) \text{ or } \mathrm{M}\ (\text{fast}) &\rightarrow \mathrm{Cu}^{*} + \mathrm{e}^{-}(\text{slow}) \text{ or } \mathrm{M}\ (\text{slow}) \end{aligned} \tag{3}$$

where e^{-} (fast) and M (fast) denote an electron and a particle having enough kinetic energy to excite Ar and/or Cu, respectively. The resulting excited species contribute to characteristic emission lines in the spectrum emitted from the breakdown zone.

The breakdown plasma zone expands upward, and it results in a plasma plume. The behavior of the plasma plume in LP-LIP varies largely by the kind and the pressure of the plasma gas: under evacuated conditions, the zone cannot be expanded so widely due to smaller collision probability, while the expansion zone is larger quenched by the surrounding gas with increasing gas pressure. The experimental configuration is reported in Fig. 2. The number density of highly energetic particles should decrease as the plasma plume expanding: therefore, excitations through the first-kind collision [Eq. (3)] take place less actively (of course, excited species having lower excitation energies would be still produced in the expansion zone). Also, some types of excited state having long lifetime could survive in the

Downloaded At: 03:00 30 January 2011

expansion zone. Excitations through the second-kind collision should be therefore considered as follows:

$$Cu + Ar^{m} \rightarrow Cu^{+} + e^{-} + Ar^{g} \quad (4)$$

$$Cu + Ar^{+} \rightarrow (Cu^{+})^{*} + Ar^{g} \quad (4')$$

where m and g denote the metastable and ground state, respectively. Equation 4′ is known as a charge-transfer collision.[22]

Typical Time-Resolved and Time-Integrated Spectra of Copper

Figure 3 shows typical LP-IPS spectra of copper in the wavelength range of 345–367 nm, both in the time-resolved mode (a) and in the time-integrated mode (b). These spectra were obtained without the blind cylinder. In the time-resolved spectra (Fig. 3a), which were measured at 400-Pa Ar, several

Downloaded At: 03:00 30 January 2011

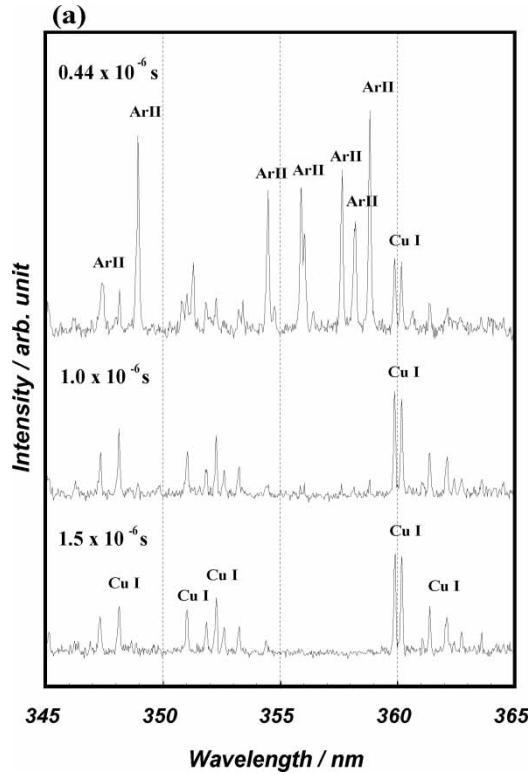

Figure 3. LP-LIP spectra of copper in the time-resolved mode (a) and the time-integrated mode (b). The time-resolved spectra are measured at 400-Pa Ar.

(continued)

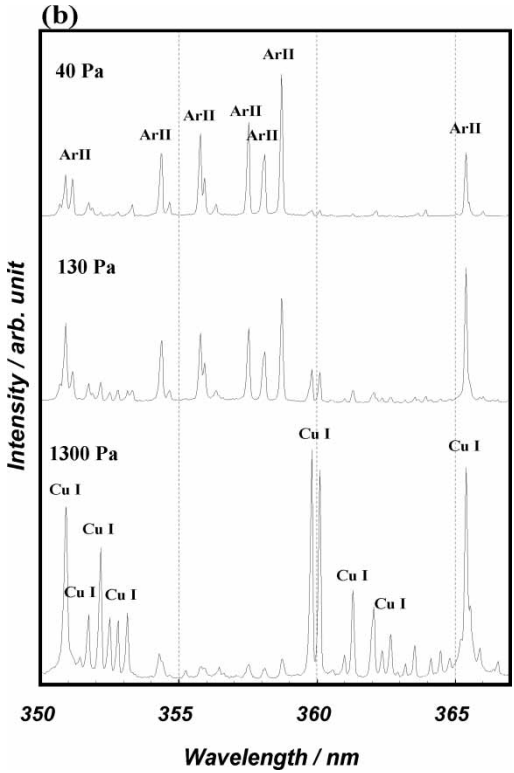

Figure 3. Continued.

Downloaded At: 03:00 30 January 2011

ionic lines of argon (Ar II) predominantly appeared just after the laser breakdown and then almost disappeared at the delay time of more than 1.0×10^{-6} s, whereas de-excitations for the copper atomic lines (Cu I) were a little delayed. It is also found from the time-integrated spectra (Fig. 3b) that the spectrum pattern is greatly varied depending on the argon pressure in the chamber, yielding increasing intensities of the Cu I lines but decreasing intensities of the Ar II lines with increasing argon pressure. These results imply that different mechanisms would play a major role in the excitation between ionic argon and atomic copper species.

Table 1 indicates that the Ar II lines require higher excitation energies (plus the ionization energy of argon atom). It is likely to consider that they are emitted mainly from the initial breakdown zone, where highly energetic particles including fast electrons are produced by coupling with the laser irradiation energy. These argon ionic species could be produced through collisions with the highly energetic particles in the breakdown zone; therefore, their emission spectra could be observed at shorter delay time. On the other hand, the Cu I lines are identified to the transitions from excited energy

Table 1. Observed emission lines and their assignment

	Assignment[a]	
Wavelength (nm)	Upper level (eV)	Lower level (eV)
Cu II 213.598	4p $^3\mathbf{F}_4$ (8.5213)	4s $^3\mathbf{D}_3$ (2.7187)
Cu II 214.897	4p $^3\mathbf{F}_3$ (8.4862)	4s $^3\mathbf{D}_3$ (2.7187)
Cu I 217.895	4p $^2\mathbf{P}_{3/2}$ (5.6882)	4s $^2\mathbf{S}_{1/2}$ (0.0000)
Cu II 219.225	4p $^3\mathbf{F}_3$ (8.4862)	4s $^3\mathbf{D}_2$ (2.8326)
Cu I 219.958	4p $^2\mathbf{D}_{5/2}$ (7.0237)	4s $^2\mathbf{D}_{5/2}$ (1.3889)
Cu I 221.459	4p $^2\mathbf{P}_{3/2}$ (6.9856)	4s $^2\mathbf{D}_{5/2}$ (1.3889)
Cu II 224.261	4p $^3\mathbf{D}_3$ (8.7830)	4s $^1\mathbf{D}_2$ (3.2563)
Cu II 224.700	4p $^3\mathbf{P}_2$ (8.2347)	4s $^3\mathbf{D}_3$ (2.7187)
Cu II 229.436	4p $^3\mathbf{P}_2$ (8.2347)	4s $^3\mathbf{D}_2$ (2.8326)
Cu I 324.735	4p $^2\mathbf{P}_{3/2}$ (3.8166)	4s $^2\mathbf{S}_{1/2}$ (0.0000)
Cu I 327.396	4p $^2\mathbf{P}_{1/2}$ (3.7858)	4s $^2\mathbf{S}_{1/2}$ (0.0000)
Cu I 351.184	7d $^2\mathbf{D}_{5/2}$ (7.3460)	4p $^2\mathbf{P}_{3/2}$ (3.8166)
Cu I 351.702	4d $^2\mathbf{F}_{5/2}$ (8.9454)	4p $^2\mathbf{F}_{5/2}$ (5.4212)
Cu I 352.277	4d $^2\mathbf{D}_{3/2}$ (8.9396)	4p $^4\mathbf{F}_{5/2}$ (5.4212)
Cu I 352.423	4d $^4\mathbf{F}_{7/2}$ (8.9382)	4p $^2\mathbf{F}_{5/2}$ (5.4212)
Cu I 352.739	4d $^4\mathbf{F}_{5/2}$ (9.0884)	4p $^2\mathbf{F}_{7/2}$ (5.5746)
Cu I 353.030	4p $^4\mathbf{F}_{5/2}$ (5.1530)	4s $^2\mathbf{D}_{3/2}$ (1.6422)
Cu I 359.914	4d $^4\mathbf{F}_{9/2}$ (8.8387)	4p $^4\mathbf{D}_{7/2}$ (5.3949)
Cu I 360.202	4d $^2\mathbf{D}_{7/2}$ (8.8359)	4p $^4\mathbf{D}_{7/2}$ (5.3949)
Cu I 361.421	4d $^4\mathbf{D}_{5/2}$ (8.9350)	4p $^4\mathbf{D}_{5/2}$ (5.5056)
Cu I 362.034	4d $^2\mathbf{F}_{7/2}$ (8.8185)	4p $^4\mathbf{D}_{7/2}$ (5.3949)
Cu I 362.734	4d $^2\mathbf{D}_{3/2}$ (8.9396)	4p $^4\mathbf{D}_{3/2}$ (5.5227)
Cu I 362.734	4d $^2\mathbf{D}_{3/2}$ (8.9396)	4p $^4\mathbf{D}_{3/2}$ (5.5227)
Cu I 365.586	4d $^2\mathbf{G}_{9/2}$ (8.7853)	4p $^4\mathbf{D}_{7/2}$ (5.3949)
Cu I 510.555	4p $^2\mathbf{P}_{3/2}$ (3.8166)	4s $^2\mathbf{D}_{5/2}$ (1.3889)
Cu I 515.323	4p $^2\mathbf{D}_{3/2}$ (6.1910)	4p $^2\mathbf{P}_{1/2}$ (3.7858)
Cu I 521.819	4d $^2\mathbf{D}_{5/2}$ (6.1919)	4p $^2\mathbf{P}_{3/2}$ (3.8166)
Ar II 348.636	4p $^2\mathbf{P}_{3/2}$ (23.801)	3d $^2\mathbf{F}_{5/2}$ (20.246)
Ar II 354.573	4d $^2\mathbf{G}_{7/2}$ (24.622)	4p $^2\mathbf{F}_{5/2}$ (21.127)
Ar II 355.690	4p $^2\mathbf{P}_{1/2}$ (21.426)	3d $^2\mathbf{P}_{1/2}$ (17.941)
Ar II 355.952	4d $^4\mathbf{F}_{7/2}$ (23.162)	4p $^3\mathbf{D}_{5/2}$ (19.680)
Ar II 357.663	4d $^4\mathbf{F}_{7/2}$ (23.014)	4p $^4\mathbf{D}_{5/2}$ (19.549)
Ar II 358.238	4d $^4\mathbf{F}_{5/2}$ (23.070)	4p $^4\mathbf{D}_{3/2}$ (19.610)
Ar II 358.846	4d $^4\mathbf{F}_{9/2}$ (22.948)	4s $^4\mathbf{D}_{7/2}$ (19.491)
Ar II 365.529	4d $^2\mathbf{F}_{5/2}$ (23.258)	4p $^2\mathbf{P}_{3/2}$ (19.867)
Ar I 415.853	5p $\mathbf{[3/2]}_2$ (14.529)	4s $\mathbf{[3/2]}_2$ (11.548)
Ar I 420.064	5p $\mathbf{[5/2]}_3$ (14.499)	4s $\mathbf{[3/2]}_2$ (11.548)

[a]Ref. [27].

levels in the neighborhood of the first ionization limit of copper atom, which might have relatively long lifetimes. These copper excited levels may be created also in the expansion zone of LP-LIP through recombination and de-excitation processes of ionized copper species initially created in

Downloaded At: 03:00 30 January 2011

the breakdown zone, which explains the delay of the Cu I emission lines. Accordingly, the time-resolved as well as the time-integrated spectra yield useful information on the excitation mechanisms of various copper lines.

Ionic Copper Emission Lines

In LP-LIPS, the $3d^9 4p$-$3d^9 4s$ transition of copper ion gives intense emission lines and their excitation energies range from 8.2 to 9.4 eV.[27] The observed Cu II lines are summarized in Table 1. Figure 4 shows intensity variations of the Cu II 214.90 nm line (8.49 eV) in the time-resolved mode (a) and the time-integrated mode (b). The time-resolved spectrum (a) is characterized by rapid reductions in the emission intensities resulting in the intensity drops down to almost zero at the delay time of more than 3.0×10^{-6} s. The

Downloaded At: 03:00 30 January 2011

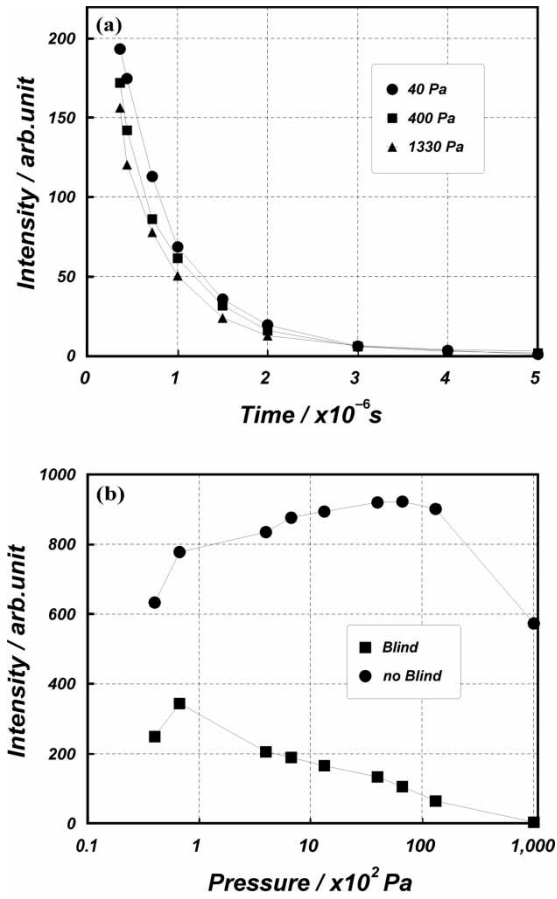

Figure 4. Intensity variations of the Cu II 214.897 nm in the time-resolved mode (a) and the time-integrated mode (b).

tendency seems to be independent of the argon pressures. The time-integrated spectrum (b) always gives much larger intensities when not using the blind cylinder compared with those with the blind, meaning that a major region for their emissions is inside the blind. These results are because the excited species of copper ion are produced mainly in the plasma breakdown zone due to collisions with highly energetic particles. Further, smaller amounts of the corresponding species are re-excited during plasma expansion after the breakdown since the number density of gas species having enough kinetic energy to excite their excited levels should decrease along with the plasma expansion. In the time-integrated measurement with the blind (Fig. 4b), the gradual decrease in the intensities is probably derived from larger quenching rate of the copper ion species by the surrounding gas along with increasing argon pressure.

Among the Cu II lines belonging to the $3d^9 4p$-$3d^9 4s$ transition, most of them showed similar intensity variations to the Cu II 214.90-nm line, except for the Cu II 224.70-nm and Cu II 229.44-nm lines. Figure 5 shows intensity variations of the Cu II 229.44-nm line (8.24 eV) in the time-resolved mode (a) and the time-integrated mode (b). Like in the Cu II 214.90-nm line, the time-resolved spectrum gives rapid reductions in the emission intensity. However, the intensities remain at the delay time of more than 3.0×10^{-6}s, especially when the pressure of argon increases. This effect means that the excitations for this Cu II line could take place in the plasma expansion zone. It should be noted that, in the time-integrated measurement (Fig. 5b), the maximum intensity appears at the argon pressure of about 1300 Pa both with and without the blind. Because this intensity maximum is observed even using the blind, it is considered that there is any excitation process, which is effective only for this particular excited level (not effective in the other excited levels), in the plasma plume followed by plasma expansion.

Downloaded At: 03:00 30 January 2011

As indicated in Table 1, both the Cu II 229.44 nm and the Cu II 224.70 nm lines are assigned to the transitions from an excited energy level ($3d^9 4p\ ^3\mathbf{P}_2$, 8.24 eV) of copper ion.[27] Several papers have reported that this excited level can be largely populated in Ar-GDP, as a selective excitation occurs through a resonance charge-transfer collision between the ground-state ion of argon and the ground-state atom of copper as follows:[18,19]

$$\mathrm{Cu} + \mathrm{Ar}^+(3p\ ^2\mathbf{P}_{3/2}, 15.94\,\mathrm{eV}) \rightarrow (\mathrm{Cu}^+)^*(4p\ ^3\mathbf{P}_2, 8.24\,\mathrm{eV}) + \mathrm{Ar}(3s\ ^1\mathbf{S}_0, 0.00\,\mathrm{eV}) + \Delta E \quad (5)$$

This type of reaction requires good matching in their excitation energies. The excitation to the $3d^9 4p\ ^3\mathbf{P}_2$ level can be selectively caused in this charge-transfer collision because the sum of the excitation energy and the ionization potential ($8.24 + 7.72 = 15.96$ eV) is very close to the ground-state energy of argon ion (15.94 eV).[27] It is expected that the charge-transfer reaction works as an additional excitation process in the expansion zone.

Because ionized argon species are derived principally from the breakdown zone, the probability of the charge-transfer collision decreases at smaller argon

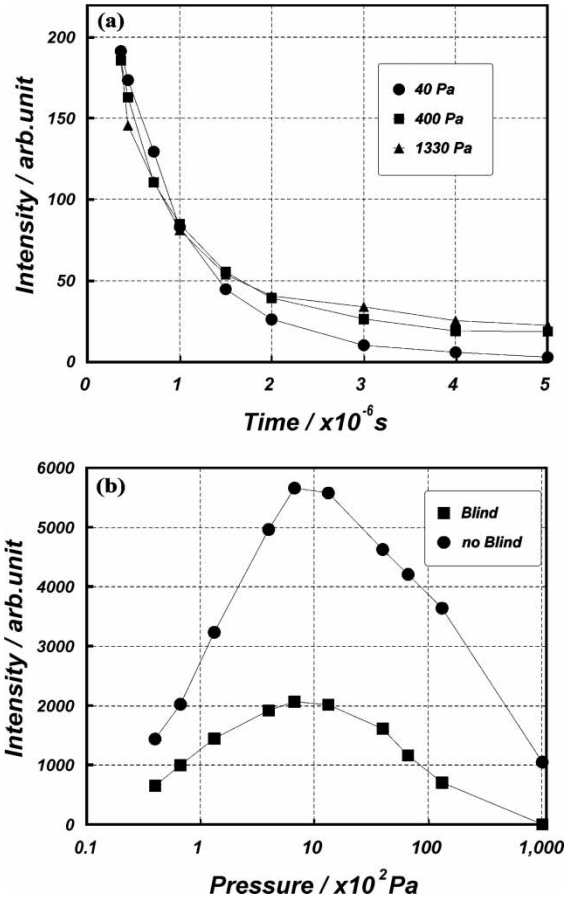

Figure 5. Intensity variations of the Cu II 229.436 nm in the time-resolved mode (a) and the time-integrated mode (b).

pressures, whereas the population of the ionized argon species is much reduced due to quenching by the surrounding gas at larger argon pressures. Therefore, the argon pressure for maximizing the Cu II intensity would be determined by a compromise condition between larger probability of the collisional ionization/excitation and greater quenching rate of argon ion species along with increasing gas pressures. The pressure dependence when the blind is used in Fig. 5(b) is considered to reveal the compromise condition.

Atomic Copper Emission Lines

Two different types of Cu I emission lines were investigated. The behavior of the Cu I 510.56-nm line (3.82 eV) are indicated in Fig. 6. Unlike in the Cu II

Downloaded At: 03:00 30 January 2011

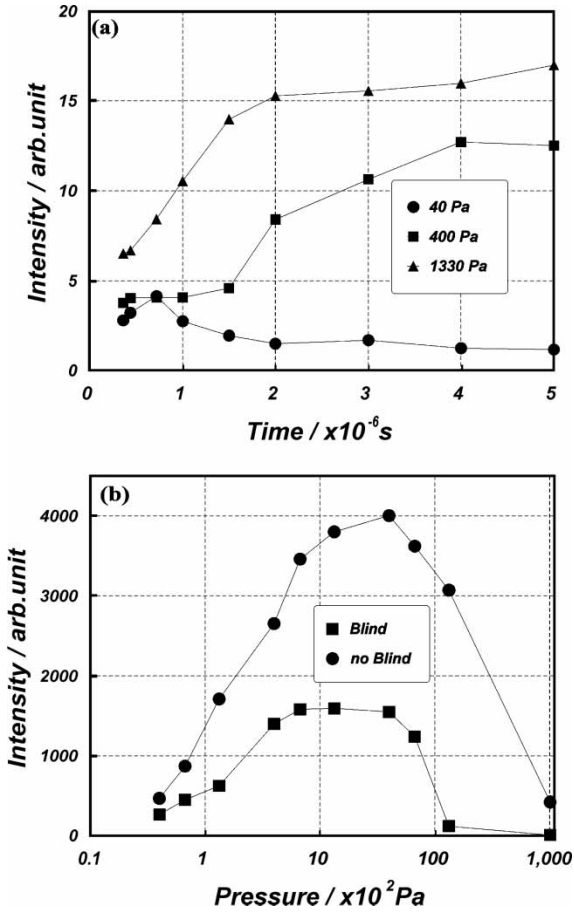

Figure 6. Intensity variations of the Cu I 510.555 nm in the time-resolved mode (a) and the time-integrated mode (b).

lines (Figs. 4 and 5), in the time-resolved measurement, there disappeared the region where strong emissions were observed immediately after the breakdown and the intensities were predominantly enhanced at prolonged delay time. This phenomena means that there are few excited species of atomic copper in the hot breakdown zone where the ionization and the overexcitation beyond atomic excited levels having smaller excitation energies may be caused. Recombination of ionic copper species and the stepwise de-excitations lead to an increased population of these low-lying excited states which enhances the emission intensities of such Cu I lines. In the time-integrated measurement (Fig. 6b), a maximum peak was found at the argon pressure of about 1300 Pa. As similar to the discussion in Cu II 229.44 nm, any re-excitation process occurring in the expansion zone would be considered for explaining this maximum peak.

Downloaded At: 03:00 30 January 2011

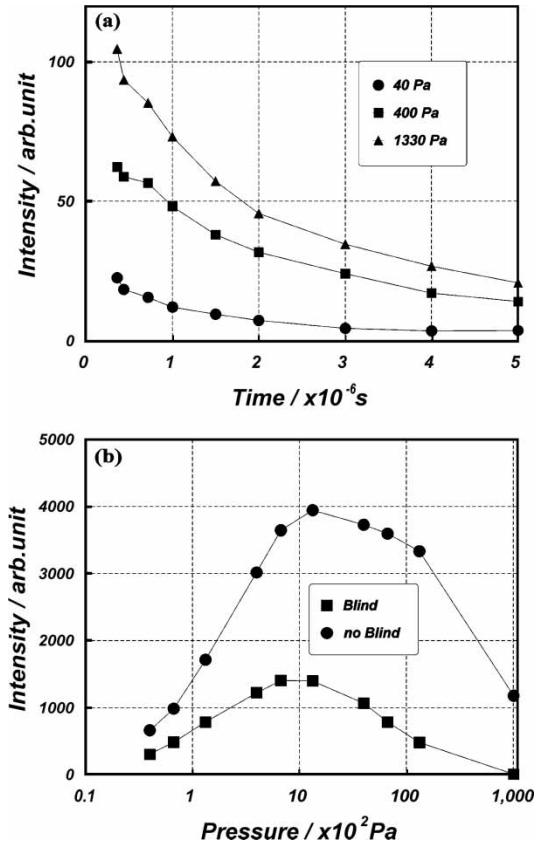

Figure 7. Intensity variations of the Cu I 219.958 nm in the time-resolved mode (a) and the time-integrated mode (b).

Figure 7 shows the results in the Cu I 291.96-nm line (7.02 eV). In the time-resolved measurement, the intensities were elevated with increasing argon pressures although they were monotonically decreased with the delay time, which was different from the data of the Cu II lines. The reason for this is that the corresponding excited species of copper atom are possibly produced by de-ionization of ionic copper species with the progress of plasma expansion. In the time-integrated measurements of this Cu I line (Fig. 7b), a maximum peak was found at the argon pressure of about 1300 Pa, as similar to in the Cu I 510.56-nm line.

Argon Emission Lines

Figure 8 shows intensity variations of the Ar II 358.85 nm line (22.95 eV) in the time-resolved mode (a) and the time-integrated mode (b). In the

Downloaded At: 03:00 30 January 2011

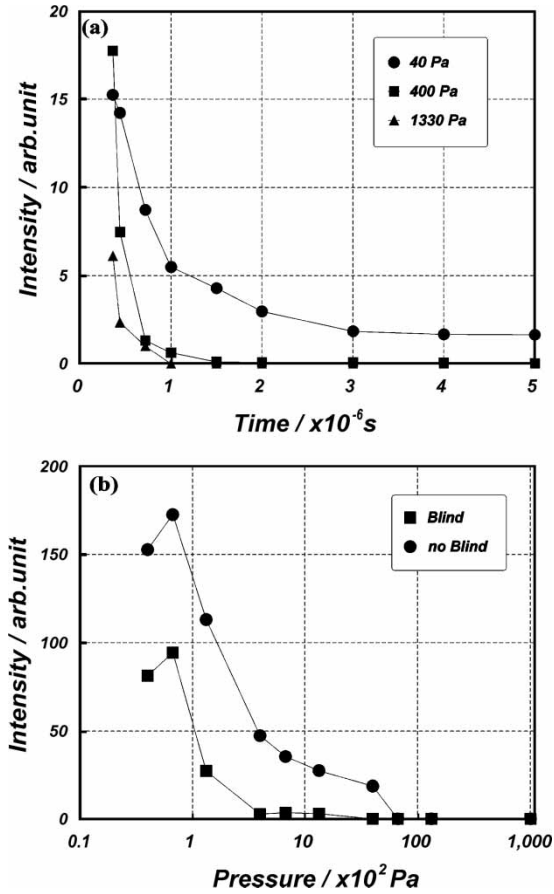

Figure 8. Intensity variations of the Ar II 358.846 nm in the time-resolved mode (a) and the time-integrated mode (b).

time-resolved measurement (a), sharp decreases in the emission intensity were observed and the intensities were not detected at the delay time of more than 1.0×10^{-6} s at the argon pressures of 400 and 1300 Pa. Furthermore, the emission intensities in the time-integrated spectrum (b) were sharply reduced along with increasing argon pressures; in the measurements with the blind, the Ar II line could not be detected at argon pressures of more than 400 Pa. This effect implies that the emission zone of the Ar II line is localized near the sample surface (the breakdown zone) where ionized species of argon requiring higher excitation energies are mainly produced. Also the recombination and de-excitation of argon ion species take place more actively at larger argon pressures.

Apart from the data of Ar II 358.85 nm, the Ar I 420.07-nm line (14.50 eV) yielded a different dependence of the emission intensity, as shown in Fig. 9.

Downloaded At: 03:00 30 January 2011

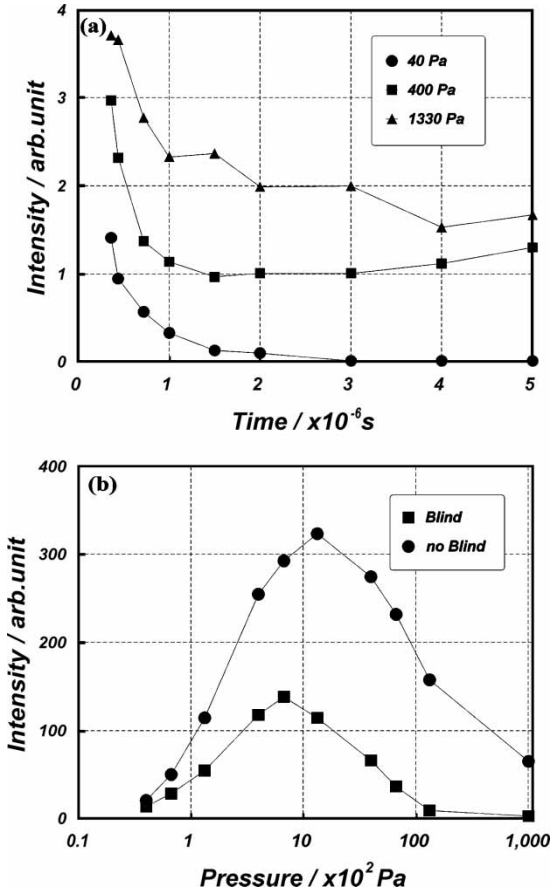

Figure 9. Intensity variations of the Ar I 420.064 nm in the time-resolved mode (a) and the time-integrated mode (b).

In the time-resolved measurement (a), the emission intensities were still observed at prolonged delay time when the argon pressure became more than 400 Pa. In the time-integrated measurement (b), a maximum peak appeared at the argon pressure of about 1300 Pa. The emissions of this Ar I line are not only from the breakdown zone but from the expansion zone, where the corresponding excited species of argon atom would be produced through the recombination process of ionic argon species.

CONCLUSIONS

In low-pressure plasma-induced plasmas, the emission intensities of copper emission lines, measured in the time-resolved and the time-integrated

Downloaded At: 03:00 30 January 2011

modes, are strongly dependent on the characteristics of copper ionic or atomic lines and their excitation energy. Also the pressure of argon plasma gas is a very important parameter for determining the behavior of these emission lines including argon lines. The excitation mechanisms in LP-LIP can be deduced from considering the relationship between the intensity variations of several emission lines and temporal and spatial variations of LIP.

ACKNOWLEDGMENTS

The authors gratefully acknowledge financial support by grants from The Iron and Steel Institute of Japan and by a grant from KAWASAKI Steel 21st Century Foundation. A part of this research is supported by Grant-in-Aids from the Ministry of Education, Science, Sports and Culture of Japan (No.15560705).

Downloaded At: 03:00 30 January 2011

REFERENCES

1. Kuzuya, M.; Murakami, M.; Maruyama, N. Quantitative analysis of ceramics by laser-induced breakdown spectrometry. *Spectrochim. Acta* **2003**, *58B*, 957–965.
2. Pu, X. Y.; Ma, W. Y.; Cheung, N. H. Sensitive analysis of aqueous colloids by laser-induced plasma spectroscopy. *Appl. Phys. Lett.* **2003**, *83*, 3416–3418.
3. Anzano, J. M.; Villoria, M. A.; Gornushkin, I. B. Laser-induced plasma spectroscopy for characterization of archaeological material. *Can. Anal. Sci. Spectosc.* **2003**, *47*, 134–140.
4. Fink, H.; Panne, U.; Niessner, R. Process analysis of recycled thermoplasts from consumer electronics by laser-induced plasma spectroscopy. *Anal. Chem.* **2002**, *74*, 4334–4342.
5. Panne, U.; Neuhauser, R. E.; Haisch, C.; Fink, H.; Niessner, R. Remote analysis of a mineral melt by laser-induced plasma spectroscopy. *Appl. Spectrosc.* **2002**, *56*, 375–380.
6. Hakkanen, H.; Houni, J.; Kaski, S.; Tommola, J. E.I.K. Analysis of paper by laser-induced plasma spectroscopy. *Spectrochim. Acta* **2001**, *56B*, 737–742.
7. Martin, M.; Cheng, M. D. Detection of chromium aerosol using time-resolved laser-induced plasma spectroscopy. *Appl. Spectrosc.* **2000**, *54*, 1279–1285.
8. Sun, Q.; Tran, M.; Smith, B. W. Direct determination of P, Al, Ca, Mn, Zn, Mg and Fe in plant material by laser-induced plasma spectroscopy. *Can. Anal. Sci. Spectrosc.* **1999**, *44*, 164–170.
9. Yoon, Y. Y.; Kim, T. S.; Chung, K. S. Application of laser induced plasma spectroscopy to the analysis of rock samples. *Analyst* **1997**, *22*, 1223–1227.
10. Naeem, T. M.; Matsuta, H.; Wagatsuma, K. Analysis of scrapped materials by low pressure laser-induced plasma spectroscopy. *ISIJ Int.* **2002**, *42*, 1318–1320.
11. Kagawa, K.; Yokoi, S. Application of the N_2 laser to laser-micro-probe spectrochemical analysis. *Spectrochim. Acta* **1982**, *37B*, 789–795.
12. Kagawa, K.; Kawai, K.; Tani, M.; Kobayashi, T. XeCl excimer laser-induced shock-wave plasma and its application to spectrochemical analysis. *Appl. Spectrosc.* **1994**, *48*, 198–205.

13. Iida, Y. Atomic emission characteristics of laser-induced plasmas in an argon atmosphere at reduced pressure. *Appl. Scpectosc.* **1989**, *43*, 229–234.
14. Iida, Y. Effects of atmosphere on laser vaporization and excitation processes of solid samples. *Spectrochim. Acta* **1990**, *45B*, 1353–1367.
15. Lee, Y. I.; Thiem, T. L.; Kim, G. H.; Teng, Y. Y.; Sneddon, J. Interaction of an excimer -laser beam with metals (3) - The effect of a controlled-atmosphere in laser-ablated plasma emission. *Appl. Spectrosc.* **1992**, *46*, 1597–1604.
16. Kurniawan, H.; Kobayashi, T.; Kagawa, K. Effects of different atmospheres on the excitation process of TEA CO_2 laser-induced shock-wave plasma. *Appl. Spectrosc.* **1992**, *46*, 581–586.
17. Grimm, W. Eine Neue Glimmentladungslampe fur die Optishe Emissionsspektral Analyse. *Spectrochim. Acta* **1968**, *23B*, 443–454.
18. Steers, E. B. M.; Fielding, R. J. Charge-transfer excitation processes in the Grimm lamp. *J. Anal. At. Spectrom.* **1987**, *2*, 239–224.
19. Wagatsuma, K.; Hirokawa, K. Spectrometric studies of excitation mechanisms on singly-ionized copper emission lines in Grimm-type glow discharge plasmas with helium mixture technique. *Spectrochim. Acta* **1991**, *46B*, 269–281.
20. Steers, E. B. M.; Leis, F. Excitation of the spectra of neutral and singly ionized atoms in the Grimm-type discharge lamp, with and without supplementary microwave plasma. *Spectrochim. Acta* **1991**, *46B*, 527–537.
21. Wagatsuma, K.; Hirokawa, K. Spectrometric studies of excitation mechanisms on singly-ionized copper emission lines in Grimm-type glow discharge plasmas with helium mixture technique. *Spectrochim. Acta* **1991**, *46B*, 269–281.
22. Dufferndach, O. S.; Black, J. G. Studies on the spectra of Cu I, Cu II, and Mn II by means of a vacuum tungsten furnace. *Phys. Rev.* **1929**, *34*, 35–43.
23. Wagatsuma, K.; Hirokawa, K. Observations of bismuth and lead ionic emission lines excited from Grimm-type glow discharge plasmas with pure neon and neon-argon mixtures. *J. Anal. At. Spectrom.* **1989**, *4*, 525–528.
24. Wagatsuma, K. Selective excitation of singly-ionized silver emission lines by Grimm glow discharge plasma using several different plasma gases. *Z. Phys.* **1996**, *D37*, 231–239.
25. Matsuta, H.; Wagatsuma, K. Emission characteristics of a low-pressure laser-induced plasma: Selective excitation of ionic emission lines of copper. *Appl. Spectrosc.* **2002**, *56*, 1165–1169.
26. Naeem, T. M.; Matsuta, H.; Wagatsuma, K. Effect of plasma gas for spectrometric analysis of tin and zinc using low-pressure laser-induced plasma. *Spectrochim. Acta* **2003**, *58B*, 891–899.
27. Moore, C. E. *Atomic Energy Levels*, Vol. 2; NBS Circular 467: Washington, DC, 1952.

Downloaded At: 03:00 30 January 2011